miRNA-205-5p can be related to T2-polarity in Chronic Rhinosinusitis with Nasal Polyps*

Mariana L.C. Silveira[1], Edwin Tamashiro[1], Anemari R. D. Santos[2], Ronaldo B. Martins[3], Francesca M. Faria[4], Lilian E. C. M. Silva[1], Raul Torrieri[2], Patrícia de C Ruy[2], Wilson A. Silva Jr[2,5], Eurico Arruda[3], Wilma T. Anselmo-Lima[1], Fabiana C. P. Valera[1]

[1] Department of Ophthalmology, Otorhinolaryngology, and Head and Neck Surgery, Ribeirão Preto Medical School, University of São Paulo, Brazil

[2] Genomics Medical Center, Clinics Hospital at Ribeirão Preto Medical School, University of São Paulo, Brazil

[3] Department of Cell and Molecular Biology and Pathogenic Bioagents, Virology Research Center, Ribeirão Preto Medical School, University of São Paulo, Brazil

[4] Department of Pathology and Legal Medicine, Ribeirão Preto Medical School, University of São Paulo, Brazil

[5] Department of Genetics, Ribeirão Preto Medical School, University of São Paulo, Brazil

Rhinology 59: 6, 567 - 576, 2021

https://doi.org/10.4193/Rhin21.109

***Received for publication:** March 24, 2021

Accepted: August 26, 2021

Abstract

Background: microRNAs (miRNAs) are directly associated with inflammatory response, but their direct role in CRSwNP (chronic rhinosinusitis with nasal polyps) remains evasive. This study aimed to compare the expression of several miRNAs in tissue samples obtained from patients with CRSwNP and controls and to evaluate if miRNAs correlate to a specific inflammatory pattern (T1, T2, T17, and Treg) or intensity of symptoms in CRSwNP.

Methods: nasal polyps (from patients with CRSwNP – n=36) and middle turbinate mucosa (from control patients – n=41) were collected. Microarray determined human mature miRNA expression, and the results obtained were validated by qPCR. miRNAs that were differentially expressed were then correlated to cytokine proteins (by Luminex), tissue eosinophilia, and SNOT-22.

Results: After microarray and qPCR analyses, six microRNAs were up-regulated in CRSwNP samples when compared with controls: miR-205-5p, miR-221-3p, miR-222-3p, miR-378a-3p, miR-449a and miR-449b-5p. All these miRNAs are directly implicated with cell cycle regulation and apoptosis, and to a minor extent, with inflammation. Importantly, miR-205-5p showed a significantly positive correlation with IL-5 concentration and eosinophil count at the tissue and with the worst SNOT-22 score.

Conclusions: miRNA 205-5p was increased in CRSwNP compared to controls, and it was especially expressed in CRSwNP patients with higher T2 inflammation (measured by both IL-5 levels and local eosinophilia) and worst clinical presentation. This miRNA may be an interesting target to be explored in patients with CRSwNP.

Key words: chronic rhinosinusitis with nasal polyps, eosinophils, IL-5, miR-205-5p, miRNA

Introduction

Chronic Rhinosinusitis (CRS), defined as inflammation of the sinonasal mucosa lasting for more than 12 weeks [(1)], is considered a significant public health problem worldwide. The Global Allergy and Asthma Network of Excellence study (GA2LEN) pointed out that 10.9% of the European countries' population present CRS [(2)]. Following the European Position Paper on Rhinosinusitis and Nasal Polyps 2012 (EPOS) criteria, Pilan et al. observed a prevalence of 5.5% of CRS in Brazil [(3)].

CRS is subdivided into two phenotypic entities: chronic rhinosinusitis with nasal polyps (CRSwNP) and chronic rhinosinusitis without nasal polyps (CRSsNP). Recently, it has been recognized

that CRS comprehends a heterogeneous group of diseases with different inflammatory and remodelling mediators [1,4–6]. The pathophysiology of CRS still is poorly understood, being both host and environmental factors implicated. The current hypotheses suggest changes in host local response (either by defective innate or adaptive immunity) and epithelial barrier (by ciliary and cell adhesion dysfunction) [7,8]. Traditionally, CRSsNP has been considered as a T1-cytokine disorder, characterized by fibrosis, and high expression of transforming growth factor- β (TGF-β), interleukin-2 (IL-2), and interferon-γ (IFN-γ), associated with increased Treg activity. Contrarywise, CRSwNP patients present a mixed inflammatory pattern: in Caucasians, there is a predominantly T2 response, characterized by edema, elevated IL-4, IL-5, and IL-13 levels, low TGF-β levels and low Treg activity [9,10], whereas Asian patients with CRSwNP have a predominant T1/T17 inflammatory pattern.

In the presence of epithelial damage (triggered by allergens, fungi, bacteria, or viruses), submucosal tissue may be exposed to external stimuli and ultimately induce the release of chemokines and cytokines [11–13]. Damage to the epithelium amplifies the immune response and, if it is strong enough, an acquired immune response ensues. The complex interaction of multiple genetic loci and various environmental exposures may explain the broad range of clinical and molecular presentation of CRS, with variable degrees of tissue inflammation and clinical symptoms, according to particular genetic and epigenetic variations.

Among all these factors, micro RNAs (miRNAs) are recognized to significantly modulate gene expression and cytokine-related functional outcomes [14].

miRNAs have a short sequence of nucleotides (20 to 22), and they are involved in the post-transcription regulation of gene expression. Altered miRNA expression is related to several human diseases, including atopic dermatitis, ulcerative colitis, allergic rhinitis, asthma, pulmonary and cardiovascular diseases, and, more recently, CRS [15,16]. miRNAs regulate several aspects of cell physiology: from development and differentiation to apoptosis, cell defense against pathogens, and inflammation. They play an essential role in recruiting immune cells, producing antibodies, and releasing inflammatory factors [12,16–18].

We hypothesized that miRNAs might influence cytokines' protein expression or clinical aspects such as disease extent or clinical impact in patients with CRSwNP.

Materials and methods

Patients with CRSwNP were prospectively recruited at Sinonasal Outpatient Clinic – Clinics Hospital of the Ribeirão Preto Medical School – University of São Paulo - from 2014 to 2017. CRSwNP diagnosis was established according to EPOS 2020 criteria [1]. Patients presenting with unilateral disease, suspected or confirmed immunodeficiencies, cystic fibrosis, or primary ciliary dyskinesia were excluded. Also, patients using corticosteroids (either topical or systemic) and macrolides within the previous month were excluded. Local IRB was obtained beforehand (file number: 35905314.4.0000.5440), and all included patients signed the informed consent.

Throughout the ENT evaluation, CRSwNP patients were instructed to fill the Sino-Nasal Outcome Test (SNOT-22) validated to the Brazilian Portuguese [19] and underwent nasal endoscopy to access Lund-Kennedy score [20] and for a nasal polyp biopsy. Two samples were collected: one was fixed in 10% buffered formalin and processed for conventional histopathological evaluation, including eosinophil counting (average of 3 representative fields in the high-power field); the other was immediately identified and frozen in liquid nitrogen, and sent to the Genomics Medical Center. All enrolled CRSwNP patients also underwent computed tomography (CT) scans for the Lund-Mackay score [20].

Patients undergoing aesthetic rhinoplasty were used as controls. The exclusion criteria were the presence of sinonasal persistent or acute nasal symptoms before the surgery and patients using corticosteroids or macrolides within one month before surgery. A biopsy from the middle turbinate was obtained for those patients during the surgical procedure, which was also frozen in liquid nitrogen and sent to Genomics Medical Center.

Total RNA, miRNA, and proteins were isolated using AllPrep DNA/RNA/miRNA/protein Universal Kit (Qiagen®), following the manufacturer's instructions. RNA and miRNAs were used in Microarray and qPCR assays, and proteins from the tissue sample were used for Luminex assays.

Microarray analysis

miRNA concentration was measured, and its quality was checked using Agilent-2100 Bioanalyzer (Agilent Technologies®).

For microarray assay, Affymetrix miRNA GeneChip 4.0 platform was used. Samples were prepared with Affymetrix® FlashTag™ Biotin HSR RNA Labeling Kit, and then they were applied to GeneRipiMatrix® miRNA Array (Affymetrix®). For this assay, 8µL of each sample and 2µL of detection oligonucleotides were added to each well. ATPmix (5 µL), Poly A Tailing Master Mix (5 µL), and FlashTag Biotin HSR Ligation Mix (4 µL) were added, and the final solution was kept at 48oC at the GeneChip cartridge for 18 hours. After the incubation, constant washings were performed to remove contaminants.

The slides were then scanned, and the raw data were quantified and analyzed at the Affymetrix® Transcriptome Analysis Console (TAC) software version 4.0.2 (https://www.thermofisher.com/br/en/home/life-science/microarray-analysis/microarray-analysis-instruments-software-services/microarray-analysis-software/affymetrix-transcriptome-analysis-console-software.html).

The analyzed array is multispecies (3770 probes for rats, mice, humans and hairpin pre-miRNAs, and 1996 probes for mature human miRNAs).

For the analysis, TAC calls differential expression analyses func-

tions from the Limma Bioconductor package (ANOVA analysis). To identify the groups to be compared in differential expression analyses, Limma uses design and contrast matrices. Contrasts between two groups (CRSwNP and control) were used in the TAC comparison. Only human mature miRNA probes were considered at this moment of analysis, with log fold change > 2 and FDR P-value < 0.05 filters.

qPCR

The differences between the groups observed at Microarray were confirmed by quantitative Polymerase Chain Reaction (q-PCR). For the qPCR study, the miR-Amp reaction was performed with 50 µL of cDNA of each patient, and samples were prepared in duplicate at 1:16 dilution. TaqMan® Advanced miRNA Assays and miRNA-specific stem-loop primers (Applied Biosystems) were used.

Polymerase chain reaction (PCR) was performed on GeneAmp® 9700 PCR System and ViiA™ 7 Real-Time PCR System: the samples were cycled at 50ºC for 2 minutes, then at 95ºC for 20 seconds, with subsequent 40 cycles of 1 second at 95ºC and 20 seconds at 60ºC. Hsa-miR-26a-5p and hsa-miR-191-5p were used as housekeeping genes. Relative gene expression was calculated using the comparative CT method by Cloud software, available online by ThermoFisher Scientific®, and data is expressed in RQ (relative quantification value). Manufactured TaqMan gene expression assay probes were used (https://www.thermofisher.com/order/genome-database/?pearUXVerSuffix=pearUX2&elcanoForm=true#!/ge/assays/ge_all/?keyword=gene%20expression&searchMethod=keyword).

Prediction of target genes and associated pathways

Following microarray and qPCR assays, we analyzed the results through the miRWalk 2.0 program (Medical Research Center – Medical Faculty Manheim, University of Heidelberg) (http://zmf.umm.uni-heidelberg.de/apps/zmf/mirwalk2/). Kyoto Encyclopedia of Genes and Genomes (KEGG) pathway (https://www.kegg.jp/kegg/pathway.html) was used to evaluate which genes and signaling pathways were the main targets for those differently expressed miRNAs. The pathways significantly correlated to miRNAs were subsequently analyzed and their relation to CRSwNP explored in the literature.

Luminex

To observe the impact of miRNA on the inflammatory profile, we correlated each differently expressed miRNA (considering both microarray and qPCR assays) to the concentration of different cytokines in patients with CRSwNP, representing the different types of immune response (1, 2 and 3).

For this purpose, the isolated protein from the tissue samples obtained from patients with CRSwNP was centrifuged for homogenization, and 50µL was used for assays. The cytokines IL-5, IL-10, IL-17, IL-33, IFN-α, IFN-γ, and TGF-ß were measured by inventoried ProcartaPlex™ immunoassay kit (eBioscience), based on Luminex® technology. Magnetic beads were prepared and added to the samples (50 µL) followed by Detection Antibodies Simplex Kits (25 µL) and Streptavidin-PE (50 µL), in duplicate. The samples were then prepared for reading (120 µL of Reading Buffer).

The expression of each miRNA (measured at qPCR) was then correlated to each cytokine's concentration (obtained at Luminex) by Pearson correlation test.

Eosinophil counting

Histopathological tissue sections were stained with hematoxylin and eosin (HE) and examined for the presence of mucosal metaplasia, edema, fibrosis, and inflammatory infiltration. Representative areas were randomly selected for eosinophil count and expressed as the number per field of 400× magnification using a Zeiss Primo Star microscope. This data was obtained from routine histopathological examination. Two pathologists (a resident and a senior doctor) assessed the sections in two different moments.

Correlation tests

We also observed the impact of differently expressed miRNAs on laboratory and clinical parameters. The expression of each miRNA was correlated to cytokine concentration, eosinophil counting, and sinonasal extension of CRS (measured by Lund-Mackay and Lund-Kennedy scores) and to clinical impact (measured by SNOT-22 score). All these analyses were performed with Pearson correlation tests and considered, at this moment, only the patients with CRSwNP.

Statistical analysis

For microarray analysis, hierarchical cluster analysis was performed, and the parametric test was employed to observe the differentially expressed miRNAs between groups. miRNAs were considered differentially expressed when their median expression showed at least 2- fold change, with FDR p-value values below 0.05.

The target genes differentially expressed at Microarray were validated by qPCR. The comparison in this analysis was performed using the unpaired t-Student test, considering P-value <0.05.

The association between the expression of miRNAs observed at qPCR and the other parameters (protein cytokine levels measured by Luminex assay, eosinophil count, SNOT-22, Lund-Kennedy and Lund-Mackay scores), Pearson correlation tests were employed.

Results

Thirty-six patients with CRSwNP (mean age of 48 ± 2.5 years, being 23 male) and 41 controls (mean age of 37 ± 2.1 years,

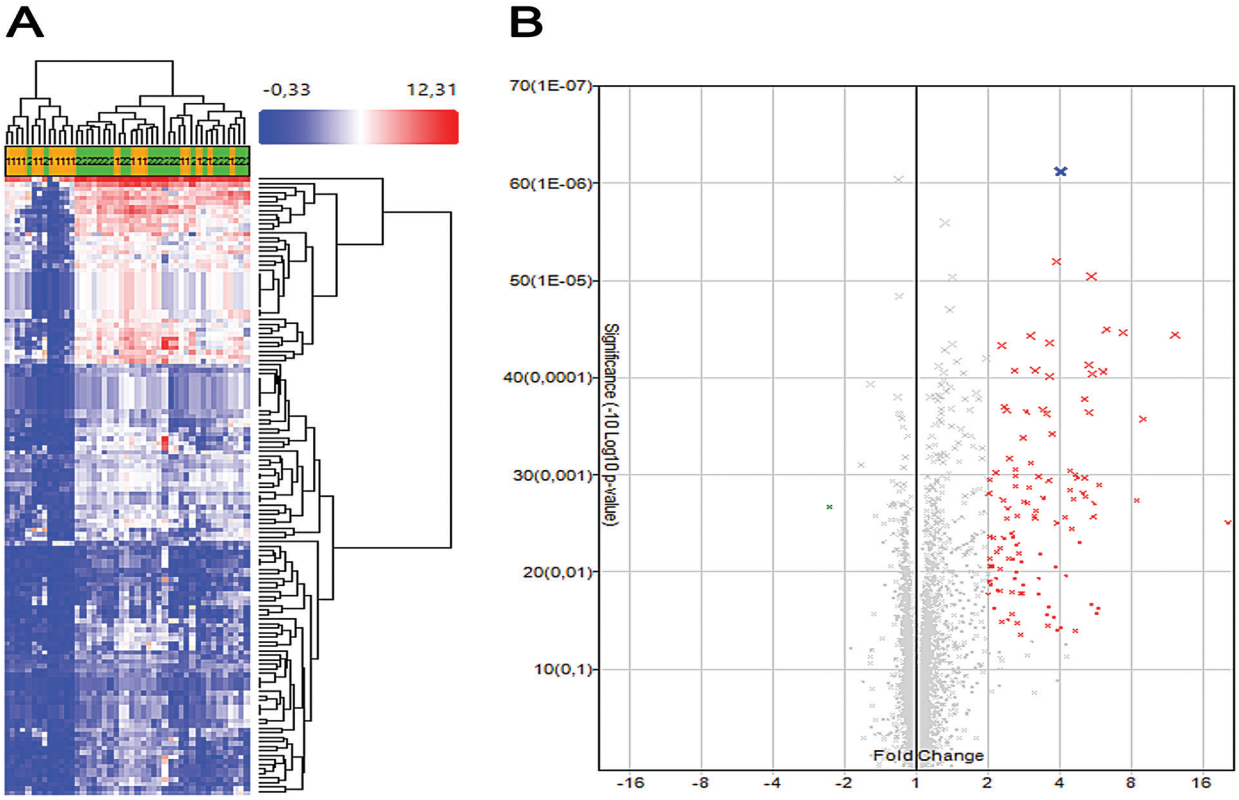

Figure 1. Microarray analysis to compare CRSwNP (n=22) and control (n=20) groups, considering all the miRNAs studied (including mature human, non-mature human and non-human probes). A) Heatmap showing all the miRNAs expressed in CRSwNP (red) and control samples (blue); B) Volcano plot showing the difference in expression between CRSwNP and controls, showing several miRNAs that were highly expressed in nasal polyps (red dots) and only one gene which expression was decreased in this group (blue dot); considering 2 logarithms as significantly different.

being 19 male) were enrolled. Among patients with CRSwNP, 8 had asthma (20.5%), one presented with Non-steroidal anti-inflammatory Exacerbated Respiratory Disease (NERD), and 5 patients were smokers (12.8%). Fourteen patients presented aeroallergen sensitization confirmed by positive prick test to mite and cockroach. Control patients did not present any nasal symptoms, and none of them presented asthma, neither positive aeroallergen sensitization; three of them were smokers.

All the samples were processed to isolate miRNAs and proteins. But after confirmation with Agilent-2100 Bioanalyzer, only 22 samples from patients with CRSwNP and 20 samples from control patients were considered to have enough miRNA concentration for microarray analysis, as we opted to assess each sample separately. Figure 1 represents the heatmap and volcano plot results obtained with microarray analysis, being all the miRNAs considered (included non-human and non-mature miRNAs). When data was analyzed with Affymetrix® TAC software and only mature human miRNAs were considered, we found a 2log difference between the groups in 16 miRNAs (hsa-miR-99b-5p, hsa-miR-205-5p, hsa-miR-221-3p, hsa-miR-222-3p, hsa-miR-320d, hsa-miR-378a-3p, hsa-miR-449a, hsa-miR-449b-5p, hsa-miR-449c-5p, hsa-miR-494-3p, hsa-miR-1246, hsa-miR-1973, hsa-miR-4429, hsa-miR-6126, hsa-miR-6836-5p and hsa-miR-7641) being all of them increased in CRSwNP samples compared to controls (Table 1). The complete microarray data analysis is deposited at www.mirbase.org.

To validate the results obtained from microarray, the following miRNAs were studied by manufactured TaqMan® Advanced assays (available at ThermoFisher® - Table 2): hsa-miR-222-3p, hsa-miR-205-5p, hsa-miR221-3p, hsa-miR-1973, hsa, miR-4429, hsa-miR-99b-5p, hsa-miR7641, hsa-miR-449a, hsa-miR-6126, hsa-miR-494-3p, hsa-miR-449b-5p, hsa-miR-378a-3p, and hsa-miR-1246, apart from the housekeeping hsa-miR-26a-5p and hsa-miR-191-5p. The results from this analysis are expressed in Table 3. For this analysis, 28 CRSwNP and 32 control samples were assessed.

The qPCR results confirmed increased expression of six of 13 miRNAs in CRSwNP in comparison to controls: hsa-miR-205-5p (2.01±1.42 in CRSwNP vs. 1.26±0.83 in controls, P-value<0.05); hsa-miR-221-3p (2.37±0.36 in CRSwNP vs. 1.49±0.17 in controls, P-value<0.05); hsa-miR-222-3p (4.86±0.86 in CRSwNP vs. 1.12±0.17 in controls, P-value<0.0001); hsa-miR-378a-3p (5.05±1.13 in CRSwNP vs. 2.33±0.75 in controls, P-value<0.05); hsa-miR-449a (1.72±0.33 in CRSwNP vs. 0.82±0.27 in controls,

Table 1. Comparative values of each miRNA transcript between CRSwNP (n=22) and controls (n=20), after microarray analysis.

Cluster ID	Transcript ID	CRSwNP (log2)	Control (log2)	Fold Change (CRSwNP vs. Control)	FDR P-value
20501176	hsa-miR-99b-5p	5.06	2.45	6.12	0.016*
20500462	hsa-miR-205-5p	7.25	4.36	7.41	0.011*
20500484	hsa-miR-221-3p	5.18	1.57	12.25	0.011*
20500486	hsa-miR-222-3p	6.18	3.52	6.32	0.011*
20509070	hsa-miR-320d	4.89	2.94	3.87	0.010*
20501243	hsa-miR-378a-3p	3.15	0.74	5.32	0.028*
20502367	hsa-miR-449a	2.46	0.6	3.64	0.016*
20504414	hsa-miR-449b-5p	2.09	0.55	2.9	0.028*
20504577	hsa-miR-449c-5p	2.54	0.65	3.72	0.036*
20503803	hsa-miR-494-3p	2.85	1.63	2.34	0.027*
20506837	hsa-miR-1246	4.18	1.02	8.98	0.030*
20510800	hsa-miR-1973	1.77	0.58	2.29	0.013*
20518801	hsa-miR-4429	3.18	1.80	2.60	0.016*
20524036	hsa-miR-6126	4.83	2.49	5.08	0.024*
20525635	hsa-miR-6836-5p	4.64	2.19	5.46	0.011*
20528493	hsa-miR-7641	7.11	4.64	5.53	0.016*

*: P-value <0.05.

Table 2. manufactured TaqMan® Advanced probes acquired at ThermoFisher Scientific® for qPCR assay.

Target Gene	Assay ID	Mature miRNA Sequence
hsa-miR-99b-5p	478343_mir	CACCCGUAGAACCGACCUUGCG
hsa-miR-205-5p	477967_mir	UCCUUCAUUCCACCGGAGUCUG
hsa-miR221-3p	477981_mir	AGCUACAUUGUCUGCUGGGUUUC
hsa-miR-222-3p	477982_mir	AGCUACAUCUGGCUACUGGGU
hsa-miR-378a-3p	478349_mir	ACUGGACUUGGAGUCAGAAGGC
hsa-miR-449a	478561_mir	UGGCAGUGUAUUGUUAGCUGGU
hsa-miR-449b-5p	479528_mir	AGGCAGUGUAUUGUUAGCUGGC
hsa-miR-494-3p	478135_mir	UGAAACAUACACGGGAAACCUC
hsa-miR-1246	483023_mir	AAUGGAUUUUUGGAGCAGG
hsa-miR-1973	478747_mir	ACCGUGCAAAGGUAGCAUA
hsa-miR-4429*	480852_mir	AAAAGCUGGGCUGAGAGGCG
hsa-miR-6126*	480186_mir	GUGAAGGCCCGGCGGAGA
hsa-miR-7641	479172_mir	UUGAUCUCGGAAGCUAAGC
Housekeeping		
hsa-miR-26a-5p	477995_mir	UUCAAGUAAUCCAGGAUAGGCU
hsa-miR-191-5p	477952_mir	CAACGGAAUCCCAAAAGCAGCUG

*: amplification was not achieved at qPCR assay

P-value<0.05); and hsa-miR-449b-5p (0.62±0.13 in CRSwNP vs. 0.30±0.05 in controls, P-value<0.05). Intriguingly, all the miRNAs observed to have different expression between groups were with increased expression in CRSwNP group when compared with control group.

The six miRNAs differently expressed between the two groups were analyzed by miRWalk 2.0 program. Subsequently, we performed an in silico analysis of genes and signaling pathways considered the primary targets for these miRNAs by KEGG pathway. The pathways that were significantly correlated to each

Table 3. Comparative values of each miRNA transcript between CRSwNP (n=32) and controls (n=28), after validation by qPCR.

Cluster ID	Transcript ID	CRSwNP (mean±SD)	Controls (mean±SD)	95% CI	P-value
20501176	hsa-miR-99b-5p	3.92±0.76	2.40±0.97	-4.04;0.99	0.23
20500462	hsa-miR-205-5p	2.01±1.42	1.26±0.83	-1.66;-0.08	0.018*
20500484	hsa-miR-221-3p	2.37±0.36	1.49±0.17	-1.66;-0.08	0.03*
20500486	hsa-miR-222-3p	4.86±0.86	1.12±0.17	-5.46;-2.02	<0.0001*
20501243	hsa-miR-378a-3p	5.05±1.13	2.33±0.75	-5.39;-0.06	0.04*
20502367	hsa-miR-449a	1.72±0.33	0.82±0.27	-1.76;-0.02	0.04*
20504414	hsa-miR-449b-5p	0.62±0.13	0.30±0.05	-1.73;-2.21	0.02*
20503803	hsa-miR-494-3p	1.96±0.90	2.2±0.46	-1.73;2.21	0.80
20506837	hsa-miR-1246	0.32±0.10	0.11±0.04	-0.43;0.01	0.06
20510800	hsa-miR-1973	2.18±0.60	1.32±0.46	-2.38;0.64	0.25
20528493	hsa-miR-7641	7.12±2.31	2.80±0.50	-9.01;0.38	0.07

*: P-value <0.05.

Table 4. the main pathways related to miRNAs found to be differently expressed between CRSwNP and control samples, according to KEGG pathway (source miRWalk 2.0 program), after P-value was adjusted.

miRNA differently expressed	Pathway Name	Adjusted P-value (BH)
hsa-miR-205-5p	Tight junction	0.0310
hsa-miR-221-3p	ErbB signaling pathway	0.0004
hsa-miR-221-3p	Axon guidance	0.0256
hsa-miR-221-3p	Renal cell carcinoma	0.0441
hsa-miR-222-3p	ErbB signaling pathway	0.0005
hsa-miR-222-3p	Axon guidance	0.0080
hsa-miR-378a-3p	Pathways in cancer	0.0016
hsa-miR-378a-3p	Colorectal cancer	0.0087
hsa-miR-449a	Endocytosis	1.11E+09
hsa-miR-449a	Axon guidance	0.0090
hsa-miR-449a	Adherens junction	0.0409
hsa-miR-449b-5p	Axon guidance	1.36E+08
hsa-miR-449b-5p	Endocytosis	0.0001

miRNA are presented at Supplementary Table 1.

The results reported by KEGG pathway showed that hsa-miR-205-5p is specially related to tight junction pathway, hsa-miR-221-3p is associated with ErbB signaling pathway, axon guidance and renal cell carcinoma, hsa-miR-222-3p is also associated with ErbB signaling pathway and axon guidance, hsa-miR-378a-3p is related to cancer, hsa-miR-449a is associated with endocytosis, axon guidance and adherens junction, and hsa-miR-449b-5p is related to endocytosis and axon guidance. The main results are represented in Table 4. As pointed here, the pathways especially implicated by those miRNAs were those related to cell cycle/ apoptosis, cell to cell signaling and axon guidance. Inflammation was not considered as the primary pathway related to those miRNAs.

We further assessed the correlation between each miRNA expression and cytokine concentration in nasal polyp tissues. For this purpose, the six differentially expressed miRNAs were individually correlated to each inflammatory cytokine concentration (IL-5, IL-10, IL-17, IL-33, IFN-α, IFN-γ, and TGF-ß). From all analyses performed, two correlations were statistically relevant at the nasal polyp tissue: a positive association between hsa-miR-205-5p expression and IL-5 concentration (R2:0.25; P-value<0.05) and a negative association between hsa-miR-449a expression and IFN-α concentration (R2: -0.20; P-value<0.05; Figure 2). All the other correlations were not different.

miRNAs expression was also correlated to the mean eosinophilia at the tissue. We observed a positive correlation between the number of eosinophils per high-power field and the expression

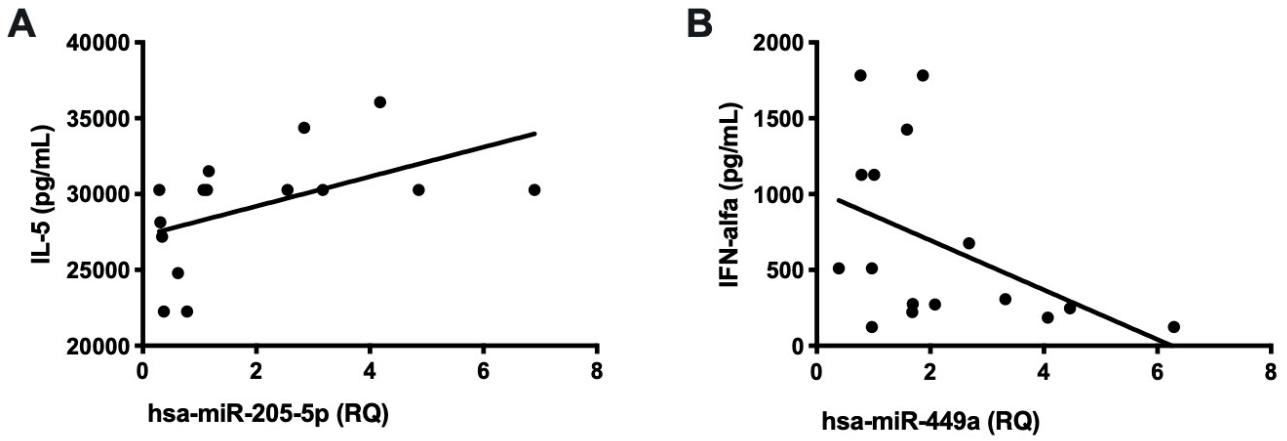

Figure 2. Pearson correlation between miRNAs and cytokines in samples from CRSwNP patients (n=32), demonstrating: A) a significant positive association between hsa-miR-205-5p (RQ) and IL-5 (pg/mL), with R2: 0.25; P-value<0.05; and B) a significant negative association between hsa-miR-449a (RQ) and IFN-α (pg/mL), with R2: -0.20; P-value<0.05.

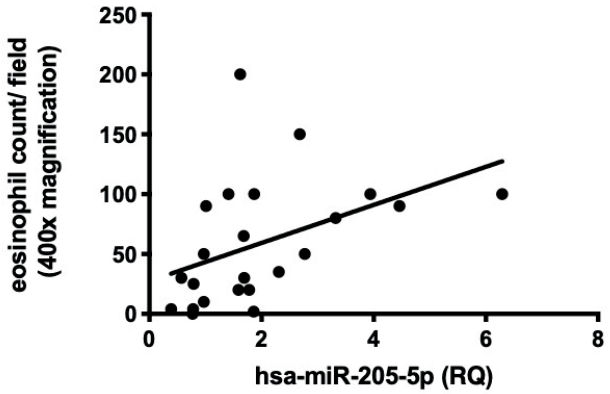

Figure 3. Pearson correlation between hsa-miR-205-5p (RQ) and eosinophil count at the tissue (by the number of eosinophils per field, 400x magnification) in samples from CRSwNP patients (n=32), showing a significant positive association, with R2: 0.16; P-value<0.05.

of hsa-miR-205-5p (R2:0.16; P-value<0.05; Figure 3). All the other correlations were not significant.

Finally, we analyzed the correlation between miRNA expression and quality of life scores (SNOT-22), nasal endoscopy findings (Lund-Kennedy score) and disease extension by CT scan (Lund-Mackay score). We observed a significant correlation between SNOT-22 score and both hsa-miR-205-5p (R2:0.20; P-value<0.05) and hsa-miR-221-3p (R2:0.27; P-value<0.01) expression, but not with the other miRNAs analyzed (Figure 4). Nevertheless, there was no significant correlation between miRNA levels and Lund-Kennedy or Lund-Mackay scores in CRSwNP patients.

Discussion

The present study evaluated the influence of miRNAs on CRSwNP by observing which miRNAs were differently expressed in nasal polyps compared to control samples and checking for correlations between miRNAs and different laboratory and clinical parameters.

Evidence indicates that miRNAs are involved in several inflammatory responses, either by influencing the profile of recruited inflammatory cells or modulating the intensity of inflammation [21]. The influence of miRNAs on sinonasal mucosa under normal and pathological conditions should be better addressed [12].

For this purpose, we prospectively compared the expression of miRNAs between CRSwNP and control patients by microarray, which was further validated by qPCR. After the analysis of both assays, the miRNAs hsa-miR-205-5p, hsa-miR-221-3p, hsa-miR-222-3p, hsa-miR-378a-3p, hsa-miR-449a and hsa-miR-449b-5p were found to be increased in CRSwNP samples compared with control.

KEGG database confirmed that the pathways most influenced by these miRNAs were related to epithelial integrity: both tight and adherens junctions are influenced respectively by miR-205-5p and miR-449a. Tight junctions (TJs) are involved in junction assembly, barrier regulation, and cell polarity, and they are essential for establishing a selectively permeable barrier through the paracellular space between neighboring cells. The epithelial barrier is described to be defective and poorly expressed in nasal polyps [8,22]. Also, TJs are highly influenced by both Th2 and Th17 cytokines [23,24] and by several external agents, such as *Staphylococcus aureus* [25] and allergens [26].

After studying Tight Junction Pathway at KEGG Pathways website (https://www.kegg.jp/kegg-bin/highlight_pathway?scale=1.0&map=map04530&keyword=tight%20junction), we observed that two other pathways are directly related to tight junctions, and they were also significantly correlated to miR-205-5p: "Adherens JUNCTION" and "Actin Cytoskeleton Regulation". Adherens junctions (AJs) are essential to maintain cell-to-cell adhesion, cell migration, wound healing and cell differentiation [27–29].

When exposed to Th2 cytokines, nasal polyps decrease E-cadherin expression, an essential adherent junction protein [23].

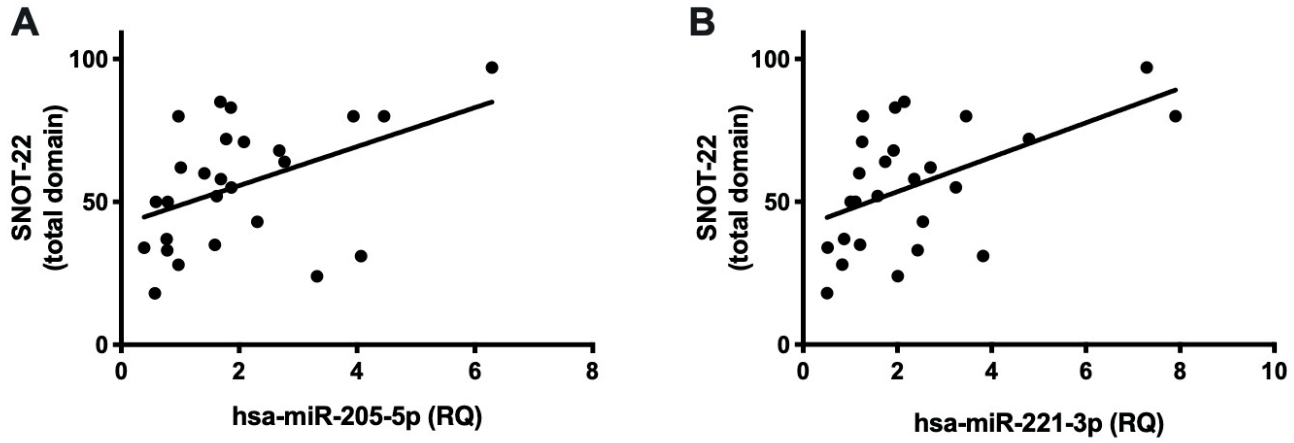

Figure 4. Pearson correlation between miRNA expression and SNOT-22 (total domain) in samples from CRSwNP patients (n=32), showing a significantly positive associations of SNOT-22 and: A) hsa-miR-205-5p (RQ), with R2: 0.20; P-value<0.05; and B) hsa-miR-221-3p (RQ), with R2: 0.27; P-value<0.01.

Decreased E-cadherin levels are specially related to epithelial barrier disruption with increasing remodeling severity, leading to goblet cell hyperplasia and basal cell proliferation, and it is associated with epithelial overgrowth and mesenchymal transition [28,30,31]. Adequate expression of miR-205 assures adequate expression of E-cadherin for maintaining the epithelial phenotype [31].

Both tight and adherens junctions are linked to the actin cytoskeleton to strengthen cell-to-cell adhesion [32]. The actin cytoskeleton, lamellipodia (an essential process for cell migration) and wound healing are all impaired in nasal polyps, and all of them are highly influenced by the presence of *Staphylococcus aureus* exoproducts [33]. Viruses can influence epithelial barriers in different ways: while rhinovirus disrupts adherens junction [34], respiratory syncytial virus disassembles junctional complexes by changing actin remodeling phosphorylation [35].

KEGG also revealed the influence of miR-221-3p and miR-222-3p on ErbB signaling pathway. Through Epithelial Growth Factor Receptor (EGFR) binding, this pathway was also related to cell proliferation and differentiation on nasal polyps [36]. Also, EGFR is related to the degranulation of goblet cells [36]. Different studies have demonstrated that the hsa-miR-221/222 cluster can regulate inflammatory airway diseases' pathogenesis, worsening inflammatory lung lesions with stimulation of TNF-α and IL-6 [37,38].

Axon guidance is a relevant pathway related to miR-221-3p, miR-222-3p miR-449a, and miR-449b-5p. Axon guidance represents a crucial stage to the neuronal network, and it is a crucial pathway to neurogenic mucosal inflammation. Signal transduction pathways downstream of these receptors converge onto the Rho GTPases to elicit changes in the cytoskeletal organization, control the assembly, disassembly, and reorganize the actin cytoskeleton [39]. Recently, axon guidance proteins were reported to be downregulated in nasal polyps [40], and *Staphylococcus aureus* has shown to negatively influence nasal polyps' lamellipodia, which is directly regulated by this pathway [33].

Finally, miR-449a and miR-449b-5p were related to the endocytosis pathway, enabling the transportation of nutrients, plasma membrane proteins, and lipids from the cell surface into the cells. B-adaptin, one of the proteins related to endocytosis, is known to be increased in aspirin-tolerant nasal polyps when compared to aspirin-sensitive individuals [41].

In summary, KEGG showed that the miRNAs increased in the present study were not directly related to the inflammatory process. Instead, they were associated with either epithelial barrier integrity, cell growth/proliferation/cytoskeletal organization, and endocytosis. Thus, it was remarkable that we found a positive association of miR-205 with IL-5 levels, polyp eosinophilia, and higher intensity of symptoms as measured by SNOT-22. Besides, we observed that patients with higher levels of miR-221-3p presented worse clinical scores measured by SNOT-22.

As miR-205-5p is not directly responsible for inducing inflammation, we believe that this positive relationship between this miRNA and T2 response observed in nasal polyps could be explained by an indirect mechanism. In fact, miR-205-5p regulates cytoskeletal organization and epithelial integrity, by tight and adherens junction production. Thus, we believe that the increase of miR-205-5p would lead to the decrease in epithelial integrity and, to induce epithelial repair, ILC2 (type-2 innate lymphoid cells) will secrete T2 cytokines, among them IL-5. The mechanisms by which ILC2 induce both epithelial repair and the expression of T2 cytokines has already been demonstrated in asthma [42] and atopic dermatitis [43].

Suojalehto et al. also observed this relationship between miR-205 and IL-5 expression in patients with allergic rhinitis [44]. Considering Suojalehto's study and ours, we can suggest that miR-205 is related to IL-5 and tissue eosinophilia regardless of whether the process is allergic or not.

Wise et al. [23] showed that Th2 cytokines compromise the

epithelial barrier. In the present study, we suggest that this may be a looped mechanism, in which miR-205, related to epithelial damage, could also lead to increased Th2 cytokines and tissue eosinophilia. E-cadherin's decrease could justify this looped relationship, inducing Th2 response in lower airway epithelial cells [45,46].

We also observed that the expression of miR-449a had a significant inverse correlation with IFN-α expression. miR-449a can induce cell differentiation and apoptosis, and this activity provides the first line of defense against genotoxic stress or virus infection [47]. Lv et al. [48] demonstrated that several viruses influence miR-34/449 family, regulating immune responses and inducing, for example, the expression of the chemokine CCL2, which is shown to be increased in CRSwNP [49]. Interestingly, in a recent article, Lewandowska-Polak et al. [50] evaluated the effect of different stimuli on wound repair in bronchial epithelial cells. They observed that regardless of the stimuli applied, lower levels of IFN-α and IFN-γ expression were related to a lower epithelial regeneration rate.

Conclusion

In summary, our results show that miRNAs that were overexpressed in CRSwNP in comparison to controls have much more action on migration, differentiation, mitosis, cellular apoptosis and cellular adhesion than on inflammation per se. Even though the inflammatory pathway was not the primary target for these genes, miRNA 205-5p was important in polarizing the T2 response on CRSwNP patients. miRNA 205-5p seems to correlate with increased IL-5 and tissue eosinophilia, along with worsening sinonasal symptoms. Altogether, our data strengths the participation of miRNA 205-5p on the pathophysiology of CRSwNP and suggests that this molecule could be an exciting target therapy in the future.

Acknowledgements

The present study was supported by FAPESP (process number: 2014/ 17572-0), by CNPq (process number 304035/2015-7), and in part by the Coordenação de Aperfeiçoamento de Pessoal de Nível Superior - Brasil (CAPES) - Finance Code 001".

Authorship contribution

MS was directly involved in all parts of the study; ET, WAS, EA and WTAL helped with the logistic to the idea, allowing use of the equipment, and discussion of results; AS helped with the microarray assay, RM with the Luminex assay, and LECMS with the PCR assay; FF analyzed the parameters in polyps' biopsies; RT and PR performed bioinformatics for the microarray and KEGG analyses; FCPV designed the study, achieved the financial support and supported and discussed all the aspects of the study. MS and FCPV were wrote the article; all co-authors read it and corrected the final manuscript.

Conflict of interest

The authors claim that there are no conflicts of interest.

Funding

Not applicable

References

1. Fokkens WJ, Lund VJ, Hopkins C, Hellings PW, Kern R, Reitsma S, et al. European Position Paper on Rhinosinusitis and Nasal Polyps 2020. Rhinology. 2020;58(Suppl S29):1-464.
2. Hastan D, Fokkens WJ, Bachert C, Newson RB, Bislimovska J, Bockelbrink A, et al. Chronic rhinosinusitis in Europe - An underestimated disease. A GA 2LEN study. Allergy. 2011;66: 1216–1223.
3. Pilan RR, Pinna FR, Bezerra TF, Mori RL, Padua FG, Bento RF, et al. Prevalence of chronic rhinosinusitis in Sao Paulo. Rhinology. 2012;50: 129–138.
4. Liao B, Liu JX, Li ZY, Zhen Z, Cao PP, Yao Y, et al. Multidimensional endotypes of chronic rhinosinusitis and their association with treatment outcomes. Allergy. 2018;73: 1459–1469.
5. Kim JW, Huh G, Rhee CS, Lee CH, Lee J, Chung JH, et al. Unsupervised cluster analysis of chronic rhinosinusitis with nasal polyp using routinely available clinical markers and its implication in treatment outcomes. Int Forum Allergy Rhinol. 2019;9: 79–86.
6. Tomassen P, Vandeplas G, van Zele T, Cardell LO, Arebro J, Olze H, et al. Inflammatory endotypes of chronic rhinosinusitis based on cluster analysis of biomarkers. J Allergy Clin Immunol. 2016;137: 1449-1456.e4.
7. Zhang Q, Wang CS, Han DM, Sy C, Huang Q, Sun Y, et al. Differential expression of Toll-like receptor pathway genes in chronic rhinosinusitis with or without nasal polyps. Acta Oto-Laryngol. 2013;133: 165–173.
8. Soyka MB, Wawrzyniak P, Eiwegger T, Holzmann D, Treis A, Wanke K, et al. Defective epithelial barrier in chronic rhinosinusitis: The regulation of tight junctions by IFN-γ and IL-4. J Allergy Clin Immunol. 2012;130: 1087-1096.e10.
9. Orlandi RR, Kingdom TT, Hwang PH, Smith TL, Alt JA, Baroody FM, et al. International Consensus Statement on Allergy and Rhinology: Rhinosinusitis. Int Forum Allergy Rhinol. 2016;6: S22–209.
10. Akdis CA, Bachert C, Cingi C, Dykewicz MS, Hellings PW, Naclerio RM, et al. Endotypes and phenotypes of chronic rhinosinusitis: A PRACTALL document of the European Academy of Allergy and Clinical Immunology and the American Academy of Allergy, Asthma & Immunology. J Allergy Clin Immunol. 2013;131: 1479–1490.
11. Kato A, Schleimer RP. Beyond inflammation: airway epithelial cells are at the interface of innate and adaptive immunity. Curr Opin Immunol. 2007;19: 711–720.
12. Sha Q, Truong-Tran AQ, Plitt JR, Beck LA, Schleimer RP. Activation of airway epithelial cells by toll-like receptor agonists. Am J Respir Cell Mol Biol. 2004;31: 358–364.
13. Laudien M, Dressel S, Harder J, Gläser R. Differential expression pattern of antimicrobial peptides in nasal mucosa and secretion. Rhinology. 2011;49: 107–11.
14. Garavelli S, de Rosa V, de Candia P. The Multifaceted Interface Between Cytokines and microRNAs: An Ancient Mechanism to Regulate the Good and the Bad of Inflammation. Front Immunol. 2018;9: 3012.
15. Zhang YN, Cao PP, Zhang XH, Lu X, Liu Z. Expression of MicroRNA machinery proteins in different types of chronic rhinosinusitis. Laryngoscope. 2012;122: 2621–2627.
16. Maes T, Tournoy KG, Joos GF. Gene therapy for allergic airway diseases. Curr Allergy Asthma Rep. 2011;11: 163–172.
17. Tomankova T, Petrek M, Gallo J, Kriegova E. MicroRNAs: Emerging Regulators of

Immune-Mediated Diseases. Scand J Immunology. 2012;75: 129–141.
18. Miller RL, Ho SM. Environmental epigenetics and asthma: Current concepts and call for studies. Vol. 177, Am J Respir Crit Care Med. 2008; 177: 567–573.
19. Kosugi EM, Chen VG, da Fonseca VMG, Cursino MMP, Neto JAM, Gregório LC. Translation, cross-cultural adaptation and validation of sinonasal outcome test (SNOT)-22 to Brazilian Portuguese. Braz J Otorhinolaryngol. 2011;77: 663–669.
20. Lund VJ, Kennedy DW. Staging for rhinosinusitis. Otolaryngol Head Neck Surg. 1997;117: S35-40.
21. O'Connell RM, Rao DS, Baltimore D. MicroRNA regulation of inflammatory responses. Vol. 30, Annu Rev Immunol. 2012;30: 295–312.
22. Jiao J, Wang C, Zhang L. Epithelial physical barrier defects in chronic rhinosinusitis. Expert Rev Clin Immunol. 2019;15: 679–688.
23. Wise SK, Laury AM, Katz EH, den Beste KA, Parkos CA, Nusrat A. Interleukin-4 and interleukin-13 compromise the sinonasal epithelial barrier and perturb intercellular junction protein expression. Int Forum Allergy Rhinol. 2014;4: 361–370.
24. Ramezanpour M, Moraitis S, Smith JLP, Wormald PJ, Vreugde S. Th17 cytokines disrupt the airway mucosal barrier in chronic rhinosinusitis. Mediators of Inflamm. 2016;2016: 9798206.
25. Murphy J, Ramezanpour M, Stach N, Dubin G, Psaltis AJ, Wormald PJ, et al. Staphylococcus Aureus V8 protease disrupts the integrity of the airway epithelial barrier and impairs IL-6 production in vitro. Laryngoscope. 2018;128: E8–15.
26. Steelant B, Farré R, Wawrzyniak P, Belmans J, Dekimpe E, Vanheel H, et al. Impaired barrier function in patients with house dust mite-induced allergic rhinitis is accompanied by decreased occludin and zonula occludens-1 expression. J Allergy Clin Immunol. 2016;137: 1043-1053.e5.
27. Georas SN, Rezaee F. Epithelial barrier function: at the front line of asthma immunology and allergic airway inflammation. J Allergy Clin Immunol. 2014;134: 509–520.
28. Kim B, Lee HJ, Im NR, Lee DY, Kang CY, Park IH, et al. Effect of matrix metalloproteinase inhibitor on disrupted E-cadherin after acid exposure in the human nasal epithelium. Laryngoscope. 2018;128: E1–7.
29. Jang YJ, Kim HG, Vitale RL, Chung PS. Localization of ZO-1 and E-cadherin in the nasal polyp epithelium. Eur Arch Oto-Rhino-Laryngology. 2002;259: 465–469.
30. Kim B, Lee HJ, Im NR, Lee DY, Kim HK, Kang CY, et al. Decreased expression of CCL17 in the disrupted nasal polyp epithelium and its regulation by IL-4 and IL-5. PLoS ONE. 2018;13: e0197355.
31. Gregory PA, Bert AG, Paterson EL, Barry SC, Tsykin A, Farshid G, et al. The miR-200 family and miR-205 regulate epithelial to mesenchymal transition by targeting ZEB1 and SIP1. Nat Cell Biol. 2008;10: 593–601.
32. Nelson WJ, Nusse R. Convergence of Wnt, -Catenin, and Cadherin Pathways. Science 2004;303: 1483–1487.
33. Valera FCP, Ruffin M, Adam D, Maillé É, Ibrahim B, Berube J, et al. Staphylococcus aureus impairs sinonasal epithelial repair: Effects in patients with chronic rhinosinusitis with nasal polyps and control subjects. J Allergy Clin Immunol. 2019;143: 591-603.e3.
34. Yeo NK, Jang YJ. Rhinovirus infection-induced alteration of tight junction and adherens junction components in human nasal epithelial cells. Laryngoscope. 2010;120: 346–352.
35. Shahriari S, Wei KJ, Ghildyal R. Respiratory syncytial virus matrix (M) protein interacts with actin in vitro and in cell culture. Viruses. 2018;10: 535.
36. Duan C, Li CW, Zhao L, Subramaniam S, Yu XM, Li YY, et al. Differential expression patterns of EGF, EGFR, and ERBB4 in nasal polyp epithelium. PLoS ONE. 2016;11: e0156949.
37. Zhao D, Zhuang N, Ding Y, Kang Y, Shi L. MiR-221 activates the NF-κB pathway by targeting A20. Biochem Biophys Res Commun. 2016;472: 11–18.
38. Galardi S, Mercatelli N, Farace MG, Ciafrè SA. NF-κB and c-Jun induce the expression of the oncogenic miR-221 and miR-222 in prostate carcinoma and glioblastoma cells. Nucleic Acids Res. 2011;39:3892–3902.
39. Hall A, Lalli G. Rho and Ras GTPases in axon growth, guidance, and branching. Cold Spring Harb perspecti Biol. 2010;2: a001818.
40. Wu D, Mueller SK, Nocera AL, Finn K, Libermann TA, Bleier BS. Axonal guidance signaling pathway is suppressed in human nasal polyps. Am J Rhinol Allergy. 2018;32: 208–216.
41. Zander KA, Saavedra MT, West J, Scapa V, Sanders L, Kingdom TT. Protein microarray analysis of nasal polyps from aspirin-sensitive and aspirin-tolerant patients with chronic rhinosinusitis. Am J Rhinol and Allergy. 2009;23: 268–272.
42. Sadik S, Lu Y, Zhu S, Cai J, Mi LL. Group 2 innate lymphoid cells (ILC2s): The spotlight in asthma pathogenesis and lung tissue injury. Allergol Immunopathol (Madr). 2021;49:208-216.
43. Zheng J, Wang X, Tao Y, Wang Y, Yu X, Liu H, et al. Yu-Ping-Feng-San ameliorates recurrent allergic inflammation of atopic dermatitis by repairing tight junction defects of the epithelial barrier. Phytomedicine. 2019;54:214-223.
44. Suojalehto H, Toskala E, Kilpeläinen M, Majuri ML, Mitts C, Lindström I, et al. MicroRNA profiles in nasal mucosa of patients with allergic and nonallergic rhinitis and asthma. Int Forum Allergy Rhinol. 2013;3: 612–620.
45. Hammad H, Lambrecht BN. Barrier epithelial cells and the control of type 2 immunity. Immunity.2015;43: 29–40.
46. Heijink IH, Kies PM, Kauffman HF, Postma DS, van Oosterhout AJM, Vellenga E. Down-Regulation of E-Cadherin in human bronchial epithelial cells leads to epidermal growth factor receptor-dependent Th2 cell-promoting activity. J Immunol. 2007 Jun;178: 7678–7685.
47. Lizé M, Herr C, Klimke A, Bals R, Dobbelstein M. MicroRNA-449a levels increase by several orders of magnitude during mucociliary differentiation of airway epithelia. Cell Cycle. 2010;9: 4579–4583.
48. Lv J, Zhang Z, Pan L, Zhang Y. MicroRNA-34/449 family and viral infections. Virus Res. 2019; 260: 1–6.
49. Ayers CM, Schlosser RJ, O'Connell BP, Atkinson C, Mulligan RM, Casey SE, et al. Increased presence of dendritic cells and dendritic cell chemokines in the sinus mucosa of chronic rhinosinusitis with nasal polyps and allergic fungal rhinosinusitis. Int Forum Allergy Rhinol. 2011;1: 296–302.
50. Lewandowska-Polak A, Brauncajs M, Jarzębska M, Pawełczyk M, Kurowski M, Chałubiński M, et al. Toll-like receptor agonists modulate wound regeneration in airway epithelial cells. Int J Mol Sci. 2018;19: pii:E2456.

Fabiana Cardoso Pereira Valera
Ribeirão Preto Medical School
University of São Paulo
Av. Bandeirantes, 3900
12º andar, Ribeirão Preto
São Paulo
Brazil, CEP – 14049-900

E-mail: facpvalera@fmrp.usp.br

This manuscript contains online supplementary material

SUPPLEMENTARY MATERIAL

Supplemantary Table 1. miRNAs that were significantly expressed between patients with CRSwNP and controls, andthe pathways thatwere significantly correlated to each miRNA.

miRNA	Pathway Name	P- value	Adjusted P-value (BH)
hsa-miR-205-5p	Tight junction	0.00020164220504626	0.031052899577124
hsa-miR-205-5p	Melanoma	0.000546753188850113	0.0825597315163671
hsa-miR-205-5p	Ubiquitin mediated proteolysis	0.000719049470031097	0.108576469974696
hsa-miR-205-5p	Phosphatidylinositol signaling system	0.000983251247943184	0.148470938439421
hsa-miR-205-5p	Pathways in cancer	0.00518380225899728	0.736099920777614
hsa-miR-205-5p	Fc gamma R mediated phagocytosis	0.00686997355704111	0.947895918953075
hsa-miR-205-5p	Small cell lung cancer	0.00695509459732491	0.950344208024843
hsa-miR-205-5p	TGF beta signaling pathway	0.00818816121501764	0.992862882608404
hsa-miR-205-5p	Endocytosis	0.00896102796619125	0.994505459192656
hsa-miR-205-5p	Adherens junction	0.0105371364351582	0.99758830087571
hsa-miR-205-5p	Non small cell lung cancer	0.0443244664887198	0.999999995951168
hsa-miR-205-5p	Inositol phosphate metabolism	0.014391239909734	0.999999995951168
hsa-miR-205-5p	SNARE interactions in vesicular transport	0.0378986245346846	0.999999995951168
hsa-miR-205-5p	Cell adhesion molecules CAMs	0.0560565407319178	0.999999995951168
hsa-miR-205-5p	Wnt signaling pathway	0.0150380589288511	0.999999995951168
hsa-miR-205-5p	Prostate cancer	0.0272035408509597	0.999999995951168
hsa-miR-205-5p	Glycosphingolipid biosynthesis lacto and neolacto series	0.0342236421190589	0.999999995951168
hsa-miR-205-5p	Regulation of actin cytoskeleton	0.0141638268570893	0.999999995951168
hsa-miR-205-5p	Glioma	0.0124084504081073	0.999999995951168
hsa-miR-221-3p	ErbB signaling pathway	3,86E+07	0.00048666739802683
hsa-miR-221-3p	Axon guidance	0.000206781767562281	0.0256409391777228
hsa-miR-221-3p	Renal cell carcinoma	0.000358773213577912	0.0441291052700832
hsa-miR-221-3p	T cell receptor signaling pathway	0.000667164543408538	0.0813940742958417
hsa-miR-221-3p	p53 signaling pathway	0.00124492293225853	0.149390751871024
hsa-miR-221-3p	Wnt signaling pathway	0.00302436785737936	0.33268046431173
hsa-miR-221-3p	Focal adhesion	0.00487191301221035	0.511550866282087
hsa-miR-221-3p	MAPK signaling pathway	0.00553348133927856	0.57548205928497
hsa-miR-221-3p	Adipocytokine signaling pathway	0.00619556171557556	0.638142856704283
hsa-miR-221-3p	Melanoma	0.00669259698900193	0.689337489867199
hsa-miR-221-3p	Gap junction	0.00719020445467722	0.732789164535147
hsa-miR-221-3p	Chronic myeloid leukemia	0.00898074515502822	0.847485027682529
hsa-miR-221-3p	Insulin signaling pathway	0.0121463191052197	0.952447540803963
hsa-miR-221-3p	Glioma	0.0159014102982927	0.974045415701016
hsa-miR-221-3p	Pathways in cancer	0.0164836997680925	0.976289759976825
hsa-miR-221-3p	Type II diabetes mellitus	0.0181321413262411	0.982670738800203
hsa-miR-221-3p	Neurotrophin signaling pathway	0.0202020634793438	0.990438886933011
hsa-miR-221-3p	Prostate cancer	0.0215301201805383	0.993914761227693
hsa-miR-221-3p	RIG I like receptor signaling pathway	0.0282596174000209	0.999630902790066
hsa-miR-221-3p	B cell receptor signaling pathway	0.0299360410734981	0.999630902790066
hsa-miR-221-3p	Pancreatic cancer	0.0299360410734981	0.999630902790066
hsa-miR-221-3p	VEGF signaling pathway	0.0353513900873365	0.999630902790066
hsa-miR-221-3p	Melanogenesis	0.0410404232641342	0.999630902790066
hsa-miR-221-3p	Phosphatidylinositol signaling system	0.03167633012918	0.999630902790066

miRNA	Pathway Name	P- value	Adjusted P-value (BH)
hsa-miR-221-3p	Colorectal cancer	0.0527283902827796	0.999630902790066
hsa-miR-221-3p	Dorso ventral axis formation	0.0378920594612102	0.999630902790066
hsa-miR-221-3p	Chemokine signaling pathway	0.0359633379092467	0.999630902790066
hsa-miR-221-3p	Endocytosis	0.0336786308973304	0.999630902790066
hsa-miR-221-3p	Cell cycle	0.0411555589796141	0.999630902790066
hsa-miR-221-3p	Calcium signaling pathway	0.0537603712742496	0.999630902790066
hsa-miR-221-3p	Fc gamma R mediated phagocytosis	0.0325356433439901	0.999630902790066
hsa-miR-222-3p	ErbB signaling pathway	4,68E+08	0.000589423179586435
hsa-miR-222-3p	Axon guidance	6,42E+09	0.00802907451374901
hsa-miR-222-3p	Renal cell carcinoma	0.000407945737677107	0.0501773257342841
hsa-miR-222-3p	T cell receptor signaling pathway	0.000771097694880707	0.0940739187754462
hsa-miR-222-3p	Wnt signaling pathway	0.00117543099413209	0.142227150289983
hsa-miR-222-3p	MAPK signaling pathway	0.00289251133187152	0.335531314497096
hsa-miR-222-3p	Insulin signaling pathway	0.00495851021934857	0.545436124128342
hsa-miR-222-3p	Focal adhesion	0.00566940743676492	0.608756977018281
hsa-miR-222-3p	p53 signaling pathway	0.00580811710834128	0.621468530592517
hsa-miR-222-3p	Melanoma	0.00734525835120303	0.749216351822709
hsa-miR-222-3p	Gap junction	0.00795905524638707	0.795905524638707
hsa-miR-222-3p	Type II diabetes mellitus	0.0194137555265322	0.995171405323066
hsa-miR-222-3p	Pathways in cancer	0.0193164706652676	0.995171405323066
hsa-miR-222-3p	Colorectal cancer	0.0565063875951489	0.999956627559655
hsa-miR-222-3p	Glioma	0.0559091933913004	0.999956627559655
hsa-miR-222-3p	Pancreatic cancer	0.0322349857203033	0.999956627559655
hsa-miR-222-3p	VEGF signaling pathway	0.0380160779191394	0.999956627559655
hsa-miR-222-3p	Fc gamma R mediated phagocytosis	0.0352875121134321	0.999956627559655
hsa-miR-222-3p	Adipocytokine signaling pathway	0.023932194795068	0.999956627559655
hsa-miR-222-3p	Dorso ventral axis formation	0.0396097791040151	0.999956627559655
hsa-miR-222-3p	Melanogenesis	0.0444129676684617	0.999956627559655
hsa-miR-222-3p	B cell receptor signaling pathway	0.0322349857203033	0.999956627559655
hsa-miR-222-3p	Chronic myeloid leukemia	0.0322349857203033	0.999956627559655
hsa-miR-222-3p	Neurotrophin signaling pathway	0.0223407056815258	0.999956627559655
hsa-miR-222-3p	Regulation of actin cytoskeleton	0.0394476441957794	0.999956627559655
hsa-miR-222-3p	Chemokine signaling pathway	0.0400154056553125	0.999956627559655
hsa-miR-378a-3p	Pathways in cancer	1,16E+09	0.00163532401630284
hsa-miR-378a-3p	Colorectal cancer	6,22E+09	0.00870129406701281
hsa-miR-378a-3p	Endometrial cancer	0.000989467738281458	0.132588676929715
hsa-miR-378a-3p	mTOR signaling pathway	0.0011104144128663	0.147685116911218
hsa-miR-378a-3p	Prostate cancer	0.00161238701278332	0.211222698674615
hsa-miR-378a-3p	Endocytosis	0.00191859965839392	0.249417955591209
hsa-miR-378a-3p	Chronic myeloid leukemia	0.00205864368598763	0.267623679178391
hsa-miR-378a-3p	Glioma	0.00366047889476839	0.468541298530354
hsa-miR-378a-3p	Insulin signaling pathway	0.00371309508174766	0.475276170463701
hsa-miR-378a-3p	Melanoma	0.00597835957736725	0.71740314928407
hsa-miR-378a-3p	Renal cell carcinoma	0.00597835957736725	0.71740314928407
hsa-miR-378a-3p	Non small cell lung cancer	0.00598536112592796	0.718243335111355
hsa-miR-378a-3p	Basal cell carcinoma	0.00654843579014452	0.765997303955835
hsa-miR-378a-3p	Hedgehog signaling pathway	0.00714897728010366	0.814983409931818

miRNA	Pathway Name	P- value	Adjusted P-value (BH)
hsa-miR-378a-3p	Neurotrophin signaling pathway	0.0178710194379667	0.986522468173567
hsa-miR-378a-3p	Progesterone mediated oocyte maturation	0.0531470092504104	0.999931671616013
hsa-miR-378a-3p	Dorso ventral axis formation	0.0359136353879573	0.999931671616013
hsa-miR-378a-3p	Nicotinate and nicotinamide metabolism	0.0359136353879573	0.999931671616013
hsa-miR-378a-3p	Lysine degradation	0.0483679844916214	0.999931671616013
hsa-miR-378a-3p	ErbB signaling pathway	0.0555849916124551	0.999931671616013
hsa-miR-378a-3p	Small cell lung cancer	0.0440554121364314	0.999931671616013
hsa-miR-449a	Endocytosis	6,69E+06	1,11E+09
hsa-miR-449a	Axon guidance	5,48E+09	0.00904887253198372
hsa-miR-449a	Adherens junction	0.000249823456529796	0.0409710468708866
hsa-miR-449a	Notch signaling pathway	0.00057701102108243	0.0934757854153536
hsa-miR-449a	Melanogenesis	0.00177791992880327	0.280911348750917
hsa-miR-449a	MAPK signaling pathway	0.00204054497340345	0.320365560824341
hsa-miR-449a	Vascular smooth muscle contraction	0.00250116007783929	0.39018097214293
hsa-miR-449a	SNARE interactions in vesicular transport	0.00258522953112528	0.403295806855543
hsa-miR-449a	Heparan sulfate biosynthesis	0.0047748412975801	0.706676512041855
hsa-miR-449a	Type II diabetes mellitus	0.0327862487498107	0.999999996806149
hsa-miR-449a	Prostate cancer	0.0238536188824814	0.999999996806149
hsa-miR-449a	Circadian rhythm mammal	0.04434755259878	0.999999996806149
hsa-miR-449a	Colorectal cancer	0.00750957009091424	0.999999996806149
hsa-miR-449a	Arrhythmogenic right ventricular cardiomyopathy ARVC	0.0423236351521036	0.999999996806149
hsa-miR-449a	Long term potentiation	0.0336435953550981	0.999999996806149
hsa-miR-449a	Melanoma	0.0131552191469991	0.999999996806149
hsa-miR-449a	Chondroitin sulfate biosynthesis	0.0105326093681782	0.999999996806149
hsa-miR-449a	Keratan sulfate biosynthesis	0.0122179035068843	0.999999996806149
hsa-miR-449a	Regulation of actin cytoskeleton	0.026779761546106	0.999999996806149
hsa-miR-449a	Pathways in cancer	0.0102401769218017	0.999999996806149
hsa-miR-449a	Phosphatidylinositol signaling system	0.00781641710656733	0.999999996806149
hsa-miR-449a	Methane metabolism	0.0501887208169574	0.999999996806149
hsa-miR-449a	Fc gamma R mediated phagocytosis	0.0186737691833497	0.999999996806149
hsa-miR-449a	Gap junction	0.0256854541066778	0.999999996806149
hsa-miR-449a	Wnt signaling pathway	0.0563284389778084	0.999999996806149
hsa-miR-449a	Chronic myeloid leukemia	0.0455228326815943	0.999999996806149
hsa-miR-449a	N Glycan biosynthesis	0.0240134356628372	0.999999996806149
hsa-miR-449a	Hypertrophic cardiomyopathy HCM	0.0436115063936624	0.999999996806149
hsa-miR-449b-5p	Axon guidance	8,06E+04	1,36E+08
hsa-miR-449b-5p	Endocytosis	7,11E+07	0.000119439131950116
hsa-miR-449b-5p	Phosphatidylinositol signaling system	0.000429298599173289	0.0704049702644194
hsa-miR-449b-5p	MAPK signaling pathway	0.000598134930065664	0.0974959936007032
hsa-miR-449b-5p	Prostate cancer	0.000727167666671358	0.11780116200076
hsa-miR-449b-5p	Notch signaling pathway	0.000872720148433315	0.140507943897764
hsa-miR-449b-5p	Pathways in cancer	0.0012765699618138	0.20169805396658
hsa-miR-449b-5p	Adherens junction	0.00139596652869545	0.220562711533881
hsa-miR-449b-5p	Chondroitin sulfate biosynthesis	0.00251837524430698	0.37523791140174
hsa-miR-449b-5p	Chronic myeloid leukemia	0.00373275905516635	0.530051785833621
hsa-miR-449b-5p	Vascular smooth muscle contraction	0.00421582182775693	0.590249907095455
hsa-miR-449b-5p	Colorectal cancer	0.00430795051513311	0.603113072118635

miRNA	Pathway Name	P- value	Adjusted P-value (BH)
hsa-miR-449b-5p	Heparan sulfate biosynthesis	0.00618711331963173	0.841447411469916
hsa-miR-449b-5p	Melanoma	0.0068878835696311	0.929864281900199
hsa-miR-449b-5p	Melanogenesis	0.00747305287848465	0.993254149842151
hsa-miR-449b-5p	Non small cell lung cancer	0.00867293295565386	0.999999999942265
hsa-miR-449b-5p	Circadian rhythm mammal	0.00853861057533534	0.999999999942265
hsa-miR-449b-5p	VEGF signaling pathway	0.0332934946829765	0.999999999942265
hsa-miR-449b-5p	B cell receptor signaling pathway	0.0261773999285652	0.999999999942265
hsa-miR-449b-5p	Acute myeloid leukemia	0.0370143179736843	0.999999999942265
hsa-miR-449b-5p	Aldosterone regulated sodium reabsorption	0.0575129115741253	0.999999999942265
hsa-miR-449b-5p	Thyroid cancer	0.0402370958585975	0.999999999942265
hsa-miR-449b-5p	Adipocytokine signaling pathway	0.016843870018625	0.999999999942265
hsa-miR-449b-5p	Methane metabolism	0.0553040573666937	0.999999999942265
hsa-miR-449b-5p	Calcium signaling pathway	0.0495399437957216	0.999999999942265
hsa-miR-449b-5p	Dorso ventral axis formation	0.0189130067237194	0.999999999942265
hsa-miR-449b-5p	Gap junction	0.035930269176333	0.999999999942265
hsa-miR-449b-5p	Galactose metabolism	0.0262377200438845	0.999999999942265
hsa-miR-449b-5p	Cell cycle	0.035850760191478	0.999999999942265
hsa-miR-449b-5p	Arrhythmogenic right ventricular cardiomyopathy ARVC	0.0559144076005228	0.999999999942265
hsa-miR-449b-5p	Fc gamma R mediated phagocytosis	0.011798267823407	0.999999999942265
hsa-miR-449b-5p	Wnt signaling pathway	0.0242844713480386	0.999999999942265
hsa-miR-449b-5p	SNARE interactions in vesicular transport	0.0132797611037964	0.999999999942265
hsa-miR-449b-5p	Keratan sulfate biosynthesis	0.0146563413923184	0.999999999942265
hsa-miR-449b-5p	Inositol phosphate metabolism	0.0253083461186731	0.999999999942265
hsa-miR-449b-5p	Hypertrophic cardiomyopathy HCM	0.0586063737541587	0.999999999942265
hsa-miR-449b-5p	Pancreatic cancer	0.0261773999285652	0.999999999942265
hsa-miR-449b-5p	Long term potentiation	0.0448320546847096	0.999999999942265
hsa-miR-449b-5p	Long term depression	0.0220840812354373	0.999999999942265
hsa-miR-449b-5p	Type II diabetes mellitus	0.0419280602029918	0.999999999942265
hsa-miR-449b-5p	N Glycan biosynthesis	0.0309730953871761	0.999999999942265
hsa-miR-449b-5p	Glioma	0.027297708219753	0.999999999942265